JACS
JOURNAL OF THE AMERICAN CHEMICAL SOCIETY
Article
pubs.acs.org/JACS

Strongly Confined HgTe 2D Nanoplatelets as Narrow Near-Infrared Emitters

Eva Izquierdo,[†] Adrien Robin,[†] Sean Keuleyan,[‡] Nicolas Lequeux,[†] Emmanuel Lhuillier,[§] and Sandrine Ithurria*[,†]

[†]Laboratoire de Physique et d'Étude des Matériaux, PSL Research University, CNRS UMR 8213, ESPCI ParisTech, 10 rue Vauquelin, 75005 Paris, France

[‡]Voxtel, Inc., and CAMCOR 1241, University of Oregon, Eugene, Oregon 97403, United States

[§]Institut des Nanosciences de Paris, CNRS-UMR 7588, Sorbonne Universités, UPMC Univ Paris 06, F-75005 Paris, France

Supporting Information

ABSTRACT: Two-dimensional colloidal nanoplatelets (NPLs), owing to the atomic-level control of their confined direction (i.e., no inhomogeneous broadening), have demonstrated improved photoluminescence (PL) line widths for cadmium chalcogenide-based nanocrystals. Here we use cation exchange to synthesize mercury chalcogenide NPLs. Appropriate control of reaction kinetics enables the 2D morphology of the NPLs to be maintained during the cation exchange. HgTe and HgSe NPLs have significantly improved optical features compared to existing materials with similar band gaps. The PL line width of HgTe NPLs (40 nm full width at half-maximum, centered at 880 nm) is a factor of 2 smaller than typical PbS nanocrystals (NCs) emitting at the same wavelength. The PL has a lifetime of 50 ns, almost 2 orders of magnitude shorter than small PbS colloidal quantum dots (CQDs), and a quantum yield of ∼10%, almost 2 orders of magnitude shorter than small PbS colloidal quantum dots (CQDs). These materials are promising for a large variety of applications spanning from telecommunications to the design of colloidal topological insulators.

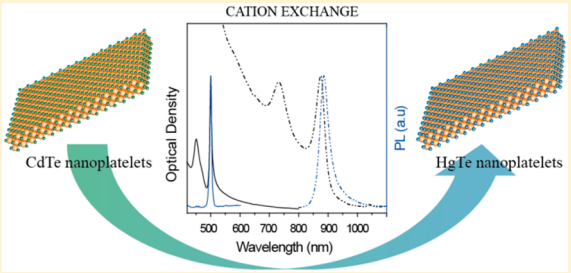

INTRODUCTION

The recent development of 2D semiconductor nanoplatelets (NPLs)[1] and quantum belts[2,3] has led to exceptional control of the optical features of cadmium chalcogenide compounds[4,5] due to the lack of inhomogeneous broadening (i.e., the ensemble spectrum is identical to the single particle emission). Their photoluminescence (PL) line widths can be as narrow as 7 nm for an emission at 500 nm. Fine control of the thickness (the confined dimension) affords tuning of the emission throughout the visible range.[5,6] The bulk band gaps of cadmium chalcogenides prevent their use in the near-infrared (IR). Therefore, narrower band gap materials need to be considered to cover this range of wavelengths. Two-dimensional colloidal lead chalcogenides have been grown using an oriented attachment of nanocrystals.[7,8] The nonuniform size of the nanocrystals, however, leads to an inhomogeneity in the NPL thickness. For the infrared range, great progress has been made with mercury chalcogenide colloidal quantum dots (CQDs).[9−11] Nevertheless, they still suffer from a limited control of their size and shape, which leads to a broadening of their optical features. In the near IR, copper indium sulfide (CIS) and PbS have received the most attention. In CIS nanocrystals, the emission relies on trap states,[12−14] which are dependent on the stoichiometry, and results in extremely broad luminescence features (full width at half-maximum (fwhm) ≈ 100 nm). Lead chalcogenide CQDs can be prepared with size polydispersity under 5%. Nonetheless, their PL line width remains relatively broad, especially for small particles emitting near 800 nm.[15] This appears to result from homogeneous broadening,[16] which leaves very little room for improvement of the synthesis. Alternative materials with better-controlled absorption and emission in the near IR are of the utmost interest.

Cation exchange[17−20] provides a way to prepare materials which cannot be directly synthesized. The process is now well established and is the most typical method used to obtain core−shell heterostructures on lead chalcogenides.[21,22] The method has also been applied to 2D NPLs by Bouet et al.[23] to obtain zinc- and lead-based NPLs from cadmium-based NPLs. However, the cation exchange fails to preserve the 2D shape of the thinnest NPLs. Kuno and colleagues have shown cation exchange on the thinnest CdSe NPLs with copper and silver, but no further exchanges were performed.[24] Using cation exchange to prepare mercury chalcogenides is actually much more difficult because of the softness of the final material, which easily results in shape reconstruction. Nevertheless, mercury cation exchange has already been reported on CdTe CQDs to grow (HgCd)Te alloys,[25−29] and on CdSe wires and magic-sized clusters to give rise to (HgCd)Se.[30,31]

Received: May 6, 2016
Published: August 3, 2016

DOI: 10.1021/jacs.6b04429
J. Am. Chem. Soc. 2016, 138, 10496−10501

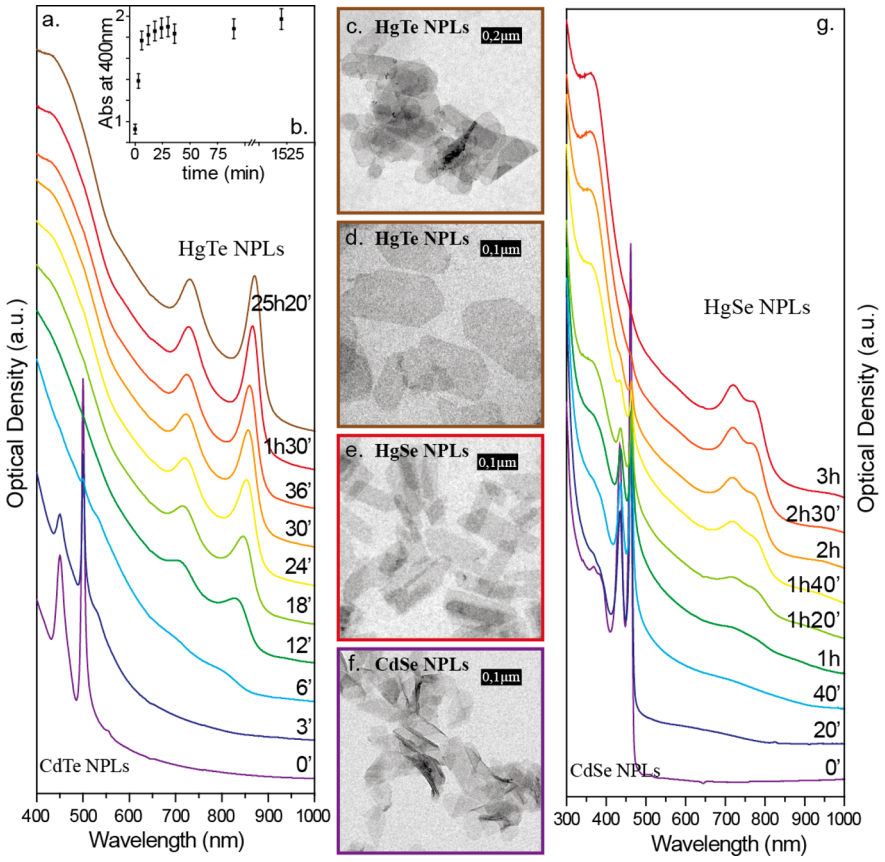

Figure 1. Absorbance spectra of the CdTe → HgTe (a) and CdSe → HgSe (g) NPLs at different times during the cation exchange reaction. The dilution remains the same for all spectra, which are offset for clarity. (b) Absorbance at 400 nm as a function of time from Figure 1a. (c and d) Transmission electron microscopy (TEM) images of the final 3 ML HgTe NPLs. (e) TEM image of 3 ML HgSe NPLs. (f) TEM image of 3 ML CdSe NPLs.

In this paper we describe a new procedure for completing mercury cation exchange to form HgTe and HgSe 2D NPLs. We use a bulky Hg precursor to slow down the reaction and obtain HgTe NPLs with exceptionally narrow near IR optical features. We attribute this to the atomically smooth 2D particles, which exhibit exceptionally high quantum confinement energies (≈1.4 eV). Similarly, the method is applied to obtain HgSe NPLs, which also present optical absorption in the near IR (≈800 nm). The integration of the HgTe NPLs into field effect transistors is also investigated and shows a switch from p-type CdTe to n-type HgTe NPLs. This work is paving the way for the development of a new generation of CQD-based optoelectronic devices with better controlled optical features in the near IR, and this work might also find some applications in the design of colloidal topological insulators.[32]

RESULTS AND DISCUSSION

Cation exchange on CdTe with Hg^{2+} to form narrow band gap HgCdTe has been proposed as a chemical path to push the absorption from the visible range to the infrared.[25] However, most of the reported methods do not lead to a complete exchange, which (i) limits the red shift of the optical feature or (ii) leads to severe inhomogeneous broadening due to the spatially inhomogeneous cation exchange.[29] To conduct a mercury cation exchange on CdTe NPLs, while preserving their 2D shape, we had to considerably slow down the reaction. Usually, copper and silver cation exchanges are performed in a homogeneous medium containing nanoparticles and a copper or silver salt. The nanoparticles are typically suspended in toluene, and the salt is dissolved in methanol.[18,33] A mixture of the two solutions leads to a quick cation exchange. In these conditions, there is no control of the speed of reaction unless the salt is introduced by slow addition.[24] Using this method with a mercury salt leads to a fast exchange and a dissolution of the NPLs. This contrasts with the same reaction conducted with spherical nanocrystals, which leads to an alloy and heterostructures.[34] We therefore used bulky precursors to slow down the reaction (see Figure S1 in Supporting Information for less bulky precursors).

Three monolayers (ML) thick CdTe NPLs (four planes of cadmium and three planes of tellurium) were synthesized according to the procedure by Pedetti et al.[35] (see Figure S2 in Supporting Information). Despite their symmetric zinc blende structure, the CdTe NPLs are strongly anisotropic, with a thickness of 1.1 nm and a lateral dimension greater than 100 nm (see Figure S3). When the solution of NPLs was mixed with $Hg(acetate)_2$ in oleylamine, a cation exchange occurred, with a typical time scale of 1 h. The exchange process was monitored by optical spectroscopy (see Figure 1a). The initial CdTe NPLs show two characteristic optical features in the visible spectrum, at 450 and 501 nm. These are attributed to the light hole and heavy hole to conduction band transitions.[5] During the cation exchange, these two peaks first disappear and slowly recover with a large red-shift in the near IR range at 735 and 882 nm. The Hg^{2+} cation exchange with 3 ML CdSe NPLs occurs similarly but at a lower rate than for the CdTe. The

DOI: 10.1021/jacs.6b04429
J. Am. Chem. Soc. 2016, 138, 10496−10501

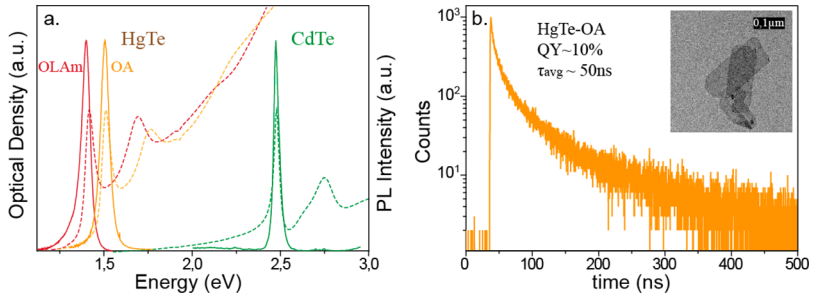

Figure 2. (a) Absorbance (dashed line) and photoluminescence (solid line) spectra of oleic acid-capped CdTe NPLs (green), oleic acid-capped HgTe NPL (OA, orange) and oleylamine-capped HgTe NPLs (OLAm, red). (b) Photoluminescence decay curve and TEM image (inset) of 3 ML oleic acid-capped HgTe NPLs. All measurements are made in solution at room temperature.

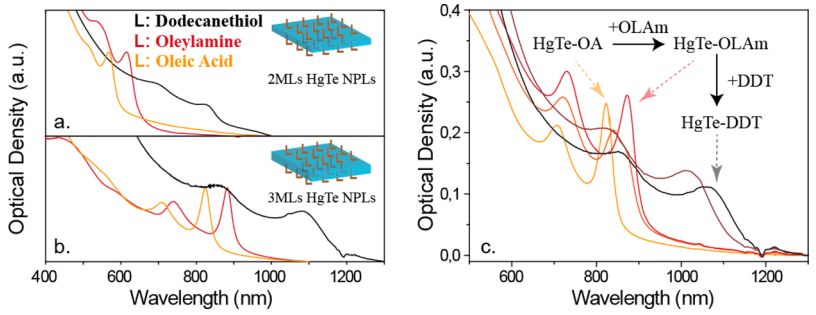

Figure 3. Absorption spectra of the oleic acid- (orange), OLAm (red)-, and dodecanethiol (black)-capped (a) 2 ML and (b) 3 ML HgTe NPLs. (c) Absorption spectra during ligand exchange from oleate (yellow) to oleylamine (red) and then to dodecanethiol (black) on 3 ML HgTe NPLs. Intermediate species are in orange and in brown.

CdSe absorption features shift from 434 and 462 nm to 719 and 766 nm, as shown in Figure 1g.

TEM images of HgTe NPLs in Figure 1c and 1d reveal that the NPL morphology and the zinc blende crystal structure are preserved after the cation exchange procedure (see Figures S3 and S4 in Supporting Information for X-ray diffraction pattern and size distribution). The final NPLs are also observed to be homogeneous in TEM contrast. After several hours, the reaction saturates and no further shift of the exciton peak is observed, as shown in Figure 1a. We attribute this observation to the complete cation exchange to cadmium-free HgTe NPLs. In these NPLs, the confinement is limited to one dimension, the thickness of the NPLs, as the lateral dimensions are larger than the 40 nm, the Bohr radius in HgTe.[36] The complete cation exchange is further confirmed by energy dispersive X-ray spectroscopy (EDX), which does not show the presence of cadmium at the end of the reaction (see Figures S5 and S6 and Table S1 in Supporting Information). Finally, we use Raman spectroscopy to confirm the complete transformation of the material (see Figure S9 in Supporting Information). Initially CdTe NPLs present one main feature at 166 cm^{-1}, which is attributed to the LO phonon mode of CdTe.[37,38] After cation exchange, this mode completely disappears and we only observe peaks assigned to HgTe[39−41] at 94 cm^{-1} (E_{TO}(Te) mode), 123 cm^{-1} (A_1(Te) mode), and 142 cm^{-1} (E_{TO}(Te) mode).[31]

In the preparation of HgSe, the shape of the NPLs is also conserved and accompanied by an unfolding of the NPLs.[42,43] This may come from a change of the surface ligands from oleic acid to oleylamine and additionally from the softness of the HgSe material. EDX analysis reveals a full exchange of the Cd to Hg (see Figures S7 and S8 and Table S2 in Supporting Information).

Absorption at short wavelength gives information on the amount and the composition of materials in solution.[44] Here we can take the quantity of materials as constant because the particle shape and size does not change during the reaction. Figure 1b gives the optical density at 400 nm as a function of time during the cation exchange reaction. We observe a large increase in the optical density over the first 10 min followed by a plateau. During this time, the CdTe absorption peaks also disappear. This suggests that the cation exchange happens in the first 10 min. Annealing of the new HgTe NPLs and reorganization of the ligands takes a longer time, as indicated by the appearance and then narrowing of the absorption structure. In addition, the photoluminescence spectra in Figure S4 in the Supporting Information show a shift of the emission maximum from 865 to 890 nm, with a reduction of the fwhm and an increase of its intensity. On the other hand, the Hg^{2+} cation exchange performed on the CdSe NPLs takes much longer. After 2 h of reaction, some CdSe NPLs remain in solution. The complete transition from CdSe to HgSe NPLs happens in approximately 3 h.

The cation exchange is explained by Pearson's theory of hard and soft acids and bases (HSAB), in which soft acids will preferentially bind to soft bases, and hard acids to hard bases. Hg^{2+} is a soft acid compared to Cd^{2+}, and by choosing the right ligands and solvents, it is then possible to favor the cation exchange.[20] In general, carboxylic acids and amines can be considered hard bases. Thus, when a soft acid such as the Hg^{2+} complexed with a hard base is introduced to a solution of CdTe nanocrystals, a cation exchange is favored. The Hg^{2+} salt is dissolved in long chain amines, which are then miscible with a solution of nanocrystals in a nonpolar solvent, such as hexane or octadecene, and form a homogeneous solution. $Hg(acetate)_2$ was chosen as the Hg^{2+} salt, as the acetate is a harder base than

DOI: 10.1021/jacs.6b04429
J. Am. Chem. Soc. 2016, 138, 10496−10501

other anions such as Cl^- in $HgCl_2$. Cation exchange did occur when $HgCl_2$ was used but at a much slower rate (see Figure S10 in Supporting Information).

In the HgTe NPLs, the confinement is so strong that we can use surface chemistry as a way to tune the optical features, while keeping the HgTe thickness unchanged. Using trioctylamine in place of oleylamine, we observe a blueshift of the transitions (see Figure 2a and Figure S11 in Supporting Information). Trioctylamine is, however, not sufficient to stabilize the HgTe NPLs in solution. As a result, additional ligands are necessary to recover a stable colloidal suspension after the cation exchange. The addition of a carboxylic acid, an amine, or a thiol leads to a suspension of NPLs, and the choice of ligand affects the absorption and emission spectra. With oleic acid, there is no shift of the absorption spectra compared to the NPLs in solution along with $Hg(acetate)_2$ in trioctylamine. The fact that oleic acid and the acetate anion both interact with the NPLs through a carboxylate, combined with the lack of change in the absorbance spectrum after the addition of oleic acid, suggests that during the cation exchange, the NPLs are capped by acetate. Small angle diffraction shows a similar interparticle distance for the CdTe and HgTe NPLs. The difference is less than 1 Å, which is smaller than the 3.2 Å thickness of a ML (see Figure S3 in Supporting Information). Addition of oleylamine leads to a red shift of the absorption spectrum to ~880 nm. Addition of thiols leads to a further red shift of ≈250 nm (see Figure 3). The strong mercury−thiol interaction favors the delocalization of the wave function into the ligands. Changes in the surface chemistry when oleic acid, oleylamine, and dodecanethiol are each added are also supported by IR spectroscopy (see Figure S12 in Supporting Information).

Small angle diffraction shows a decrease in the interparticle spacing of approximately 1 nm when oleylamine is added after oleic acid. We attribute this change to a difference in packing density and interdigitation of the two ligands.

One of the most striking features of the HgTe NPLs is that their optical features are exceptionally narrow. The PL line width for ensemble measurement is 57 meV (less than 40 nm) for an emission peak at 887 nm (1.40 eV) for oleylamine-capped NPLs (see Figure 2a). For oleic acid-capped NPLs, the PL signal is maximum at 828 nm (1.50 eV). Monodisperse PbS CQDs with similar peak emission wavelengths have a fwhm at least twice those observed here for HgTe NPLs.[15] In fact, even the emission line width of a single PbS CQD is broader (100 ± 30 meV).[16] This observation is even more striking because of the semimetal nature of bulk HgTe (i.e., zero bulk optical band gap). This means that the band gap energy is entirely a result of quantum confinement.[44] The fact that the fwhm remains narrow after the cation exchange reflects that no roughness is introduced in the confined direction.

The HgTe NPLs exhibit an emission quantum yield on the order of 10% with an average lifetime of 50 ns (Figure 2b and Figure S13 in Supporting Information). This lifetime is also much shorter than for lead chalcogenides[45−47] and CIS[13] CQDs, which have PL lifetimes in the microsecond range. This observation is consistent with the previous observation that for CdSe NPLs the PL emission lifetime was found to be shorter than for spherical particles of the same composition and band gap energy.[5]

This cation exchange may also be applied to 2 ML CdTe NPLs, leading to HgTe NPLs with optical features in the visible and the near IR (Figure 3a). Again a dependence of the absorption peak wavelengths on the ligands is observed. With 2 ML HgTe NPLs, capped with oleic acid, the first excitation absorption peak appears at 568 nm. However, the oleylamine capping leads to a peak at 615 nm. Ligand exchange from oleylamine to dodecanethiol leads to a large red shift of more than 170 nm (Figure 3a). Two ML dodecanethiol-capped HgTe NPLs have the first absorption peak at the same wavelength as 3 ML oleic acid-capped HgTe NPLs. Sulfide has a strong affinity for mercury, and the addition of sulfide on both surfaces of the 2 ML HgTe NPLs is apparently similar to the addition of a half ML on both sides. Subsequent ligand exchanges from oleic acid to oleylamine, and then from oleylamine to dodecanethiol, can be monitored by absorption spectroscopy, as shown for 3 ML HgTe NPLs in Figure 3b.

Finally, we investigate how the transport properties of the NPLs are affected by the cation exchange. To efficiently gate the system, we use ion gel gating, which has several advantages such as (i) large tunability of the carrier density,[48] (ii) in-air measurements, and (iii) low bias (<3 V) operation.[49] We first conduct a solution-phase ligand exchange to promote S^{2-} capping[50] to increase the inter-NPL coupling. Then we use $LiClO_4$ in polyethylene glycol as the ion gel electrolyte (see part 8 of Supporting Information for details). The initial CdTe contains only p-type II−VI semiconductor nanocrystals.[49] After cation exchange, the HgTe NPLs behave as n-type semiconductors (see Figure 4 and Figure S14 in Supporting Information) and the conductance is typically a factor of 50 higher than for a CdTe NPL film of similar thickness. In narrow band gap materials, such as HgTe, the carrier density n is thermally activated and therefore follows an Arrhenius behavior, $n \propto \exp(-E_a/k_bT)$. In intrinsic materials, the activation energy is half the band gap. During the cation exchange process, the band gap decreases by 800 meV, which is responsible for the observed rise in the conductance. For similar surface chemistry and gating, HgTe CQDs were previously observed to be ambipolar.[49,51] Here we use S^{2-} as the capping ligand, which tends to form an HgS surface layer. Moreover, HgS CQDs were recently reported to be stably n-doped.[52] We thus believe that the formation of this n-type surface layer is responsible for the observed switch in the majority carrier during the cation exchange.

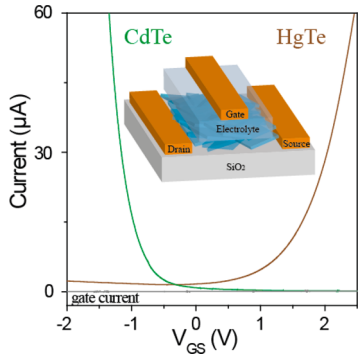

Figure 4. Drain and gate current as a function of gate voltage for an electrolyte-gated thin film of CdTe (green) and HgTe (brown) NPLs. Measurements are made at room temperature. The gate bias is stepped in 1 mV increments. The drain-source bias is 0.5 V for CdTe and 10 mV for HgTe.

DOI: 10.1021/jacs.6b04429
J. Am. Chem. Soc. 2016, 138, 10496−10501

CONCLUSIONS

We report the synthesis of 2D HgTe NPLs via a cation exchange procedure starting with CdTe NPLs and using a mercury amine complex. We show that the cation exchange is complete (i.e., the final material is Cd-free) and has exceptionally narrow near IR optical features. The fwhm can be as small as 57 meV for ensemble emission centered near 890 nm. Because of the extreme confinement energy in this system, we show that surface chemistry can be used to tune the band gap, which reflects the partial delocalization of the wave function into the ligand shell. Finally, we build an electrolytic transistor and show that the conductivity switches from p-type in CdTe to n-type in HgTe.

In addition to the bright and fast near IR luminescence of this material, we believe these results are a promising first step to building 2D colloidal topological insulators.[53,54] In particular, theory predicts HgTe QD-based honeycomb lattice structures would have a Dirac cone and nontrivial band gap, but this remains unconfirmed due to the difficulties in preparing such materials.[55]

ASSOCIATED CONTENT

Supporting Information

The Supporting Information is available free of charge on the ACS Publications website at DOI: 10.1021/jacs.6b04429.

Details of CdTe and CdSe NPLS synthesis; details of cation exchange with different mercury precursors; absorption and emission spectroscopies of HgTe NPLS; energy dispersive X-ray spectroscopy (EDS), Raman spectroscopy, X-ray diffraction patterns of NPLs; lifetime measurements of HgTe NPLs; infrared spectroscopy of HgTe NPLS capped with different ligands; ligand exchange and fabrication of field effect transistors (PDF)

AUTHOR INFORMATION

Corresponding Author

*sandrine.ithurria@espci.fr

Notes

The authors declare no competing financial interest.

ACKNOWLEDGMENTS

We thank Thomas Pons for fruitful discussions. We thank the SBPC (Réseau des Salles Blanches Paris Centre) for Raman spectroscopy. We thank the Agence National de la Recherche for funding through grants Nanodose and H2DH. This work has been supported by the Region Ile-de-France in the framework of DIM Nano-K. This work was supported by French state funds managed by the ANR within the Investissements d'Avenir programme under reference ANR-11-IDEX-0004-02 and more specifically within the framework of the Cluster of Excellence MATISSE.

REFERENCES

(1) Lhuillier, E.; Pedetti, S.; Ithurria, S.; Nadal, B.; Heuclin, H.; Dubertret, B. *Acc. Chem. Res.* **2015**, *48*, 22.

(2) Joo, J.; Son, J. S.; Kwon, S. G.; Yu, J. H.; Hyeon, T. *J. Am. Chem. Soc.* **2006**, *128*, 5632.

(3) Liu, Y. H.; Wayman, V. L.; Gibbons, P. C.; Loomis, R. a.; Buhro, W. E. *Nano Lett.* **2010**, *10*, 352.

(4) Ithurria, S.; Dubertret, B. *J. Am. Chem. Soc.* **2008**, *130*, 16504.

(5) Ithurria, S.; Tessier, M. D.; Mahler, B.; Lobo, R. P. S. M.; Dubertret, B.; Efros, A. L. *Nat. Mater.* **2011**, *10*, 936.

(6) Wang, F.; Wang, Y.; Liu, Y.-H.; Morrison, P. J.; Loomis, R. a; Buhro, W. E. *Acc. Chem. Res.* **2015**, *48*, 13.

(7) Schliehe, C.; Juarez, B. H.; Pelletier, M.; Jander, S.; Greshnykh, D.; Nagel, M.; Meyer, A.; Foerster, S.; Kornowski, A.; Klinke, C.; Weller, H. *Science* **2010**, *329*, 550.

(8) Morrison, P. J.; Loomis, R. a.; Buhro, W. E. *Chem. Mater.* **2014**, *26*, 5012.

(9) Kershaw, S. V.; Susha, A. S.; Rogach, A. L. *Chem. Soc. Rev.* **2013**, *42*, 3033.

(10) Kovalenko, M. V.; Kaufmann, E.; Pachinger, D.; Roither, J.; Huber, M.; Stangl, J.; Hesser, G.; Schäffler, F.; Heiss, W. *J. Am. Chem. Soc.* **2006**, *128*, 3516.

(11) Lhuillier, E.; Keuleyan, S.; Liu, H.; Guyot-Sionnest, P. *Chem. Mater.* **2013**, *25*, 1272.

(12) Pons, T.; Pic, E.; Lequeux, N.; Cassette, E.; Bezdetnaya, L.; Guillemin, F.; Marchal, F.; Dubertret, B. *ACS Nano* **2010**, *4*, 2531.

(13) Li, L.; Pandey, A.; Werder, D. J.; Khanal, B. P.; Pietryga, J. M.; Klimov, V. I. *J. Am. Chem. Soc.* **2011**, *133*, 1176.

(14) Van der Stam, W.; Bladt, E.; Rabouw, F. T.; Bals, S.; De Mello Donega, C. *ACS Nano* **2015**, *9*, 11430.

(15) Hendricks, M. P.; Campos, M. P.; Cleveland, G. T.; Jen-La Plante, I.; Owen, J. S. *Science* **2015**, *348* (6240), 1226.

(16) Peterson, J. J.; Krauss, T. D. *Nano Lett.* **2006**, *6*, 510.

(17) Son, D. H.; Hughes, S. M.; Yin, Y.; Alivisatos, P. A. *Science* **2004**, *306* (5698), 1009.

(18) Beberwyck, B. J.; Surendranath, Y.; Alivisatos, P. A. *J. Phys. Chem. C* **2013**, *117*, 19759.

(19) Miszta, K.; Gariano, G.; Brescia, R.; Marras, S.; De Donato, F.; Ghosh, S.; De Trizio, L.; Manna, L. *J. Am. Chem. Soc.* **2015**, *137*, 12195.

(20) De Trizio, L.; Manna, L. *Chem. Rev.* **2016**, DOI: 10.1021/acs.chemrev.5b00739.

(21) Pietryga, J. M.; Werder, D. J.; Williams, D. J.; Casson, J. L.; Schaller, R. D.; Klimov, V. I.; Hollingsworth, J. a. *J. Am. Chem. Soc.* **2008**, *130*, 4879.

(22) Lambert, K.; De Geyter, B.; Moreels, I.; Hens, Z. *Chem. Mater.* **2009**, *21*, 778.

(23) Bouet, C.; Laufer, D.; Mahler, B.; Nadal, B.; Heuclin, H.; Pedetti, S.; Patriarche, G.; Dubertret, B. *Chem. Mater.* **2014**, *26*, 3002.

(24) Wang, Y.; Zhukovskyi, M.; Tongying, P.; Tian, Y.; Kuno, M. *J. Phys. Chem. Lett.* **2014**, *5*, 3608.

(25) Kershaw, S. V.; Burt, M.; Harrison, M.; Rogach, A.; Weller, H.; Eychmuller, A. *Appl. Phys. Lett.* **1999**, *75*, 1694.

(26) Smith, A. M.; Nie, S. *J. Am. Chem. Soc.* **2011**, *133*, 24.

(27) Wang, H.; Lou, S.; Tang, Z.; Xu, W.; Shang, H.; Shen, H.; Li, L. S. *Dalt. Trans.* **2012**, *41*, 12726.

(28) Gupta, S.; Zhovtiuk, O.; Vaneski, A.; Lin, Y.-C.; Chou, W.-C.; Kershaw, S. V.; Rogach, A. L. *Part. Part. Syst. Char.* **2013**, *30*, 346.

(29) Smith, A. M.; Lane, L. A.; Nie, S. *Nat. Commun.* **2014**, *5*, 4506.

(30) Antanovich, A.; Prudnikau, A.; Gurin, V.; Artemyev, M. *Chem. Phys.* **2015**, *455*, 32.

(31) Prudnikau, A.; Artemyev, M.; Molinari, M.; Troyon, M.; Sukhanova, A.; Nabiev, I.; Baranov, A. V.; Cherevkov, S. a.; Fedorov, A. V. *Mater. Sci. Eng., B* **2012**, *177*, 744.

(32) Ando, Y. *J. Phys. Soc. Jpn.* **2013**, *82* (10), 1.

(33) Son, D. H.; Hughes, S. M.; Yin, Y.; Alivisatos, P. A.; Hee, D.; Son, D. H.; Hughes, S. M.; Yin, Y.; Alivisatos, P. A. *Science* **2004**, *306*, 1009.

(34) Taniguchi, S.; Green, M.; Lim, T. *J. Am. Chem. Soc.* **2011**, *133*, 3328.

(35) Pedetti, S.; Nadal, B.; Lhuillier, E.; Mahler, B.; Bouet, C.; Abécassis, B.; Xu, X.; Dubertret, B. *Chem. Mater.* **2013**, *25*, 2455.

(36) Rinnerbauer, V.; Hingerl, K.; Kovalenko, M.; Heiss, W. *Appl. Phys. Lett.* **2006**, *89*, 1.

(37) Islam, S. S.; Rath, S.; Jain, K. P.; Abbi, S. C.; Julien, C.; Balkanski, M. *Phys. Rev. B: Condens. Matter Mater. Phys.* **1992**, *46*, 4982.

DOI: 10.1021/jacs.6b04429
J. Am. Chem. Soc. 2016, 138, 10496−10501

(38) Amirtharaj, P. M.; Pollak, F. H. *Appl. Phys. Lett.* **1984**, *45*, 789.
(39) Pine, a. S.; Dresselhaus, G. *Phys. Rev. B* **1971**, *4*, 356.
(40) Brodsky, M. H.; Gambino, R. J.; Smith, J. E.; Yacoby, Y. *Phys. Status Solidi B* **1972**, *52*, 609.
(41) Ingale, A. *Phys. Rev. B* **1989**, *40*, 353.
(42) Bouet, C.; Mahler, B.; Nadal, B.; Abecassis, B.; Tessier, M. D.; Ithurria, S.; Xu, X.; Dubertret, B. *Chem. Mater.* **2013**, *25*, 639.
(43) Hutter, E. M.; Bladt, E.; Goris, B.; Pietra, F.; van der Bok, J. C.; Boneschanscher, M. P.; Donega, C. D. M.; Bals, S.; Vanmaekelbergh, D. *Nano Lett.* **2014**, *14*, 6257.
(44) Lhuillier, E.; Keuleyan, S.; Guyot-Sionnest, P. *Nanotechnology* **2012**, *23*, 175705.
(45) Clark, S. W.; Harbold, J. M.; Wise, F. W. *J. Phys. Chem. C* **2007**, *111*, 7302.
(46) Kovalenko, M. V.; Schaller, R. D.; Jarzab, D.; Loi, M. a.; Talapin, D. V. *J. Am. Chem. Soc.* **2012**, *134*, 2457.
(47) De Geyter, B.; Justo, Y.; Moreels, I.; Lambert, K.; Smet, P. F.; Van Thourhout, D.; Houtepen, A. J.; Grodzinska, D.; De Mello Donega, C.; Meijerink, A.; Vanmaekelbergh, D.; Hens, Z. *ACS Nano* **2011**, *5*, 58.
(48) Lhuillier, E.; Pedetti, S.; Ithurria, S.; Heuclin, H.; Nadal, B.; Robin, A.; Patriarche, G.; Lequeux, N.; Dubertret, B. *ACS Nano* **2014**, *8*, 3813.
(49) Lhuillier, E.; Ithurria, S.; Descamps-Mandine, A.; Douillard, T.; Castaing, R.; Xu, X. Z.; Taberna, P. L.; Simon, P.; Aubin, H.; Dubertret, B. *J. Phys. Chem. C* **2015**, *119*, 21795.
(50) Nag, A.; Kovalenko, M. V.; Lee, J.; Liu, W.; Spokoyny, B.; Talapin, D. V. *J. Am. Chem. Soc.* **2011**, *133*, 10612.
(51) Liu, H.; Keuleyan, S.; Guyot-Sionnest, P. *J. Phys. Chem. C* **2012**, *116*, 1344.
(52) Jeong, K. S.; Deng, Z.; Keuleyan, S.; Liu, H.; Guyot-Sionnest, P. *J. Phys. Chem. Lett.* **2014**, *5*, 1139.
(53) König, M.; Wiedmann, S.; Brüne, C.; Roth, A.; Buhmann, H.; Molenkamp, L. W.; Qi, X.; Zhang, S. *Science* **2007**, *318*, 766.
(54) Bernevig, A. B.; Hughes, T. L.; Zhang, S. *Science* **2006**, *314*, 1757.
(55) Beugeling, W.; Kalesaki, E.; Delerue, C.; Niquet, Y.-M.; Vanmaekelbergh, D.; Smith, C. M. *Nat. Commun.* **2015**, *6*, 6316.

DOI: 10.1021/jacs.6b04429
J. Am. Chem. Soc. 2016, 138, 10496−10501